Published in final edited form as:

Cancer Res. 2015 September 15; 75(18): 3788–3799. doi:10.1158/0008-5472.CAN-15-0054.

IL-17 Promotes Mammary Tumor Progression by Changing the Behavior of Tumor Cells and Eliciting Tumorigenic Neutrophils Recruitment

Luciana Benevides[1], **Denise Morais da Fonseca**[1], **Paula Barbim Donate**[1], **Daniel Guimarães Tiezzi**[2], **Daniel D De Carvalho**[3], **Jurandyr M de Andrade**[2], **Gislâine A Martins**[4], **João S Silva**[5]

[1]Department of Biochemistry and Immunology, Ribeirão Preto Medical School, University of São Paulo, Ribeirão Preto, São Paulo, Brazil

[2]Department of Gynecology and Obstetrics, Breast Disease Division, Ribeirão Preto Medical School, University of São Paulo, Ribeirão Preto, São Paulo, Brazil

[3]Ontario Cancer Institute, Princess Margaret Cancer Centre, University Health Network, and Department of Medical Biophysics, University of Toronto, Toronto, Canada

[4]F. Widjaja Foundation Inflammatory Bowel and Immunobiology Research Institute and Department of Medicine and Biomedical Science, Cedars-Sinai Medical Center, Los Angeles, California

[5]Department of Biochemistry and Immunology, Ribeirão Preto Medical School, University of São Paulo, Ribeirão Preto, São Paulo, Brazil

Abstract

The aggressiveness of invasive ductal carcinoma (IDC) of the breast is associated with increased IL17 levels. Studying the role of IL17 in invasive breast tumor pathogenesis, we found that metastatic primary tumor-infiltrating T lymphocytes produced elevated levels of IL17, whereas IL17 neutralization inhibited tumor growth and prevented the migration of neutrophils and tumor cells to secondary disease sites. Tumorigenic neutrophils promote disease progression, producing CXCL1, MMP9, VEGF, and TNFα, and their depletion suppressed tumor growth. IL17A also induced IL6 and CCL20 production in metastatic tumor cells, favoring the recruitment and differentiation of Th17. In addition, IL17A changed the gene-expression profile and the behavior of nonmetastatic tumor cells, causing tumor growth *in vivo*, confirming the protumor role of IL17.

Corresponding Author: Av. Bandeirantes, 3900 – 14049-900 – Ribeirão Preto – São Paulo – Brazil, Phone/Fax: (55) 16-3602 3234, jsdsilva@fmrp.usp.br.

Authors' Contributions

Conception and design: L. Benevides, D.M. da Fonseca, G.A. Martins, J.S. Silva
Development of methodology: L. Benevides, D.G. Tiezzi, J.M. de Andrade
Acquisition of data (provided animals, acquired and managed patients, provided facilities, etc.): L. Benevides, J.M. de Andrade
Analysis and interpretation of data (e.g., statistical analysis, biostatistics, computational analysis): L. Benevides, P.B. Donate, D.D. De Carvalho, J.M. de Andrade, G.A. Martins, J.S. Silva
Writing, review, and/or revision of the manuscript: L. Benevides, D.G. Tiezzi, J.M. de Andrade, G.A. Martins, J.S. Silva
Administrative, technical, or material support (i.e., reporting or organizing data, constructing databases): D.M. da Fonseca
Study supervision: G.A. Martins, J.S. Silva

Disclosure of Potential Conflicts of Interest

No potential conflicts of interest were disclosed.

Furthermore, high IL17 expression was associated with lower disease-free survival and worse prognosis in IDC patients. Thus, IL17 blockade represents an attractive approach for the control of invasive breast tumors.

Introduction

Breast cancer continues to be one of the leading causes of cancer-associated deaths among women worldwide (1). The initiation of breast cancer is likely caused by a combination of oncogenic mutations that promote genetic instability and accelerated cellular proliferation (2). Cancer develops in a complex host–tissue microenvironment that comprises immune cells, fibroblasts, and blood and lymphatic vessels (3). In the tumor microenvironment, inflammatory mediators, such as the cytokines IL1, IL6, and TGFβ, stimulate cancer cell proliferation and invasion and contribute to disease progression (4).

IL17 is the major effector cytokine produced by Th17 cells, a subtype of T helper cell. Th17 differentiation is mediated by a combination of signaling via IL6, IL21, IL1β, IL23, and TGFβ through the intracellular signaling molecule STAT3, which induces expression of the transcription factor Rorγt (5). Th17 plays active roles in inflammation and autoimmune disease and appears to be important in pulmonary bacterial immunity as well as protection against infection by certain protozoa (6, 7). Although IL17 has been detected in several tumors, such as prostate, gastric, lung and colon cancers, and lymphoma (8–13), whether the role of IL17 is pro- or antitumoral remains controversial, and its function seems to depend on the cancer type (14). IL17 acts in several cell types and leads to the production of GM-CSF, IL1, IL6, TNFα, chemokines, activation of NOS2 and metalloproteinases, and leukocyte recruitment (6, 15). Therefore, we hypothesized that IL17 is a key cytokine in tumor pathogenesis and modulates tumor progression. In fact, we demonstrated that IL17A production is increased in patients with invasive ductal carcinoma (IDC) of the breast and that tumor-infiltrating IL17A-producing cells are positively correlated with the presence of regulatory T (Treg) cells in the tumor microenvironment, as well as with tumor aggressiveness and a poor disease prognosis (16). These data prompted us to investigate how IL17 affects invasive tumor progression. Herein, using a metastatic (4T-1) and nonmetastatic (67NR) murine mammary tumor model, we demonstrated that IL17A was produced by tumor-infiltrating $CD4^+$ T lymphocytes during metastatic tumor progression, and that the neutralization of IL17 inhibited tumor growth and prevented the migration of tumorigenic neutrophils and metastasis. Moreover, IL17 had a direct effect on 4T-1 tumor cells by stimulating the release of IL6 and CCL20. In addition, IL17 altered the gene-expression profile in 67NR tumor cells associated with tumor growth. High expression of IL17 was also associated with lower disease-free survival (DFS) and worse prognosis in patients with IDC. Thus, our study uncovers a previously unknown, key role for IL17 in tumor progression by changing the behavior of tumor cells and eliciting tumorigenic neutrophil recruitment.

Materials and Methods

Human subjects and study populations

Tumor biopsies and peripheral blood samples were obtained from 23 patients with IDC of the breast who received care at the Department of Gynecology and Obstetrics, Breast Disease Division, Ribeirão Preto School of Medicine, University of São Paulo, from 2008 to 2010. The inclusion criteria included patients with IDC of the breast who had not received prior therapy for cancer. Control skin biopsy samples were obtained from women undergoing cosmetic breast and abdominoplasty surgeries. All subjects signed an informed consent form releasing the use of their specimens before participating in the study. This study was approved by the Ethics Committee of the Ribeirão Preto Medical School Hospital.

Murine model of mammary carcinoma

Specific pathogen-free, 8- to 10-week-old female BALB/c mice were obtained from a local breeding facility at the University of São Paulo, Brazil. Mice were injected with 50 μL of a single-cell suspension containing 5×10^4 of a 4T1 mouse metastatic mammary tumor cell line (purchased from the ATCC) or 67NR nonmetastatic mammary tumor cell line provided by Jing Yang (University of California, San Diego, San Diego, CA) orthotopically into the fourth mammary fat pad, as described previously (17). The sizes of the primary tumors were assessed morphometrically using electronic calipers. Tumor volumes were calculated according to the following formula: tumor volume (mm^3) = $L \times W^2/2$, where L represents the major axis (largest cross-sectional diameter) of the tumor, and W represents the minor axis. The data are presented as the mean + SE (mean ± SEM). For the treatment with goat anti-mouse IL17, antigen affinity-purified polyclonal antibody (AF-421-NA; R&D Systems), the mice received 5 doses of 10 μg of anti-IL17 antibody by i.p. injection, beginning 6 days after tumor-cell inoculation (days postinoculation, dpi) and every 3 days thereafter. To deplete neutrophils, the mice received 5 doses of 30 μg of rat anti-mouse Ly6G (1A8; Biolegend) antibody by i.p injection, from 18 dpi and every 3 days thereafter. For the treatment with rat anti-mouse IL6 antibody (MP5-20F3; BioXcell), the mice received 5 doses of 20 μg of anti-IL6 antibody by i.p. injection, and treatment was initiated at 1 dpi and every 4 days thereafter. Lung and tumor tissue specimens were routinely embedded in paraffin and stained with hematoxylin and eosin (H&E) to assess the presence of metastatic colonies. In total, 4-μm H&E-stained sections from at least three different levels were examined. All procedures were performed in accordance with the International Guidelines for the Use of Animals and by the local Ethics Committee at the University of São Paulo, Brazil.

Gene-expression measurement by quantitative real-time PCR

Total RNA isolation and real quantitative real-time PCR (qPCR) analyses were conducted as detailed in Supplementary Data. The primers are listed in Supplementary Table S1. The analyses were performed using the cycle threshold (C_t) method, which allows for quantitative analysis of the expression of a factor using the formula $2^{-\Delta\Delta}C^t$, in which ΔC_t = C_t target gene—C_t of the housekeeping gene GAPDH (glyceraldehyde phosphate dehydrogenase) or β-actin, and $\Delta\Delta C_t = \Delta C_t$ sample—ΔC_t.

Microarray analysis

To assess the gene-expression profiles of the biopsies of patients with breast tumors and 67NR and 4T-1 tumor cell lines, RNA was isolated and microarray analyses were conducted as detailed in Supplementary Data.

Immunohistochemistry analysis

Frozen breast tumor tissue sections (5 μm) were prepared and subjected to immunohistochemistry analysis using the antibodies described in Supplementary Data.

Isolation of leukocytes and cell culture

To characterize the inflammatory infiltrate in the tumors, lung, and spleen, cells were isolated tissue as described in Supplementary Data. Mononuclear cells isolated from murine mammary tumors were stimulated with PMA (50 ng/mL) plus ionomycin (500 ng/mL; Sigma) for 4 hours in 48-well plates. Lung cells were stimulated *in vitro* with ultrapure LPS (100 ng/mL; Invivogen) for 6 hours in 24-well plates. For all conditions, brefeldin A (BD Biosciences) was added during the last 2 hours for the determination of intracellular cytokines by flow cytometry. Splenocytes from mice were stimulated with anti-CD3 (2 μg/mL) plus anti-CD28 antibody (1 μg/mL; BD Biosciences) for 72 hours to measure the IL17 and IFNγ levels in the supernatants by ELISA. The murine mammary tumor cell lines 4T1 and 67NR were treated with recombinant murine IL17A (rIL17; 400 ng/mL; Biosource) in 24-well plates. After 48 hours, IL6 and CCL20 levels were measured in the supernatants by ELISA, the cells were collected, and the mRNA was extracted to evaluate the gene expression by qPCR.

Flow-cytometry assay

For T-cell analysis, antibodies to the following mouse proteins were obtained from BD Biosciences: CD3 (145-2C11), CD4 (RM4-5), CD8, (53–6.7), TCR γδ (UC7-13D5), IL17A (TC11-18H10), and IFNγ (XMG1.2) or their respective isotype controls (BD Biosciences). For neutrophil analysis, antibodies to the following mouse proteins were obtained from Biolegend: CD11b (M1/70), F4/80 (BM8), MHCII (M5/114.15.2), Ly6G (1A8), and TNFα (MP6-XT22). Intracellular cytokine staining was performed according to the manufacturer's instructions (BD Biosciences). Data acquisition was performed using the FACSCanto II and analyzed according to size based on forward-scatter and granulosity by side-scatter dot plots using the FlowJo software.

FACS-based cell sorting

For FACS, single-cell suspensions from spleens and tumors obtained from 4T-1 tumor-bearing mice were isolated and stained, and the $Ly6G^{+}F4/80^{-}$ cells were identified by gating on $CD11b^{hi}MHCII^{-}$ cells. Sorting was performed with an Aria FACS (BD Biosciences), and the pelleted cells were added directly to TRIzol reagent for gene-expression analysis.

Air pouch model

Air pouches were created in the dorsal side of the back of BALB/c. PBS, CCL20 (400 ng), and 4T1 or 67NR supernatant were injected into the air pouch; 20 hours later, the cell

infiltrates were harvested by pouch lavage and stimulated with PMA (50 ng/mL) plus ionomycin (500 ng/mL; Sigma) for 4 hours, and brefeldin A (BD Biosciences) was added during the last 2 hours to determine the intracellular IL17 by flow cytometry.

Statistical analysis

The statistical analysis was performed using an unpaired *t* test or ANOVA followed by Bonferroni multiple comparison tests. Kaplan–Meier curves were used to assess the influence of immune parameters on DFS. The significance of these parameters was calculated using the log-rank test (5.0 GraphPad Software). All values were considered significantly different at $P < 0.05$.

Results

Metastatic primary tumor-infiltrating lymphocytes produce IL17A

To investigate the role of IL17A in the pathogenesis of invasive breast cancer, we injected 4T1 metastatic mouse mammary tumor cells into the mammary fat pads of BALB/c mice. The 4T1 cells line grows rapidly at the primary site and forms metastasis in the lung, liver, bone, and brain, which makes this cell line an excellent model for studying the progression of breast cancer (17). To better characterize IL17-associated responses in the 4T1 tumor model, we evaluated the kinetics of IL17A and IFNγ production by tumor-infiltrating lymphocytes (TIL) isolated from mice with metastatic (4T-1) and nonmetastatic (67NR) tumors. We found that, as early as 15 dpi with tumor cells, 4T-1 TILs produced high levels of IL17A compared with 67NR TILs (Fig. 1A), whereas both produced similar levels of IFNγ. To assess the kinetics of IL17A and IFNγ production during the metastatic tumor development, the cytokine levels in the supernatants of total splenocytes were evaluated. We found that the maximum peak of IL17A production occurred at 15 and 25 dpi, whereas the production of IFNγ peaked at 25 dpi (Fig. 1B). In addition, the levels of IL17A were 15-fold higher after tumor induction. To determine the cellular source of these cytokines, leukocytes were isolated from the tumor microenvironment and stimulated with PMA and ionomycin. We found that $CD3^+CD4^+$, $CD3^+CD8^+$, and $CD3^+\gamma\delta^+$T cells produced IL17A and IFNγ at all assessed points (Fig. 1C and D). In particular, we observed an increase in the number of IL17A-producing $CD3^+CD4^+$ and $TCR\gamma\delta^+$ T cells at 25 and 35 dpi, whereas the number of $IL17^+CD8^+$ T cells was only slightly elevated at 25 dpi (Fig. 1C). However, we found increased numbers of IFNγ-producing $CD3^+CD8^+$ and $TCR\gamma\delta^+$ T cells at 35 dpi, whereas the numbers of $CD3^+CD4^+IFN\gamma^+$ T cells were maintained throughout the entire period (Fig. 1D). Together, these data reveal that IL17A is produced by $CD3^+CD4^+$ (Th17) and $TCR\gamma\delta^+$ T cells during metastatic primary tumor growth.

IL17 promotes tumor growth and controls neutrophil recruitment

To further investigate whether IL17A is involved in the pathogenesis of invasive breast cancer, we treated 4T-1–inoculated BALB/c mice with anti–IL17-neutralizing antibody and analyzed tumor progression. 4T-1–inoculated mice treated with anti-IL17A antibodies showed a significant reduction in tumor volume in comparison with mice treated with an IgG control (Fig. 2A). The tumor volumes in the 4T-1–inoculated and anti–IL17-treated mice were similar to those of mice injected with 67NR tumors (Fig. 2A). Similarly, TC-1–

bearing C57BL/6 mice treated with anti-IL17 antibodies showed a significant reduction of tumor volume (Supplementary Fig. S1). In addition, anti-IL17 treatment led to 100% of survival (as assessed on day 50 dpi) in mice inoculated with a metastatic mammary tumor, in comparison with 80% of mortality of the 4T-1 tumor-inoculated BALB/c mice (Fig. 2B). All animals that survived up to 50 dpi were sacrificed due the large size of their primary tumor. Moreover, the administration of anti–IL17A–neutralizing antibodies significantly reduced tumor mass (Fig. 2C) and size in tumor-bearing mice (Fig. 2D), which was accompanied by a decreased polymorphonuclear cells migration compared with the control mice (Fig. 2E). To assess whether IL17 favors disease progression, we analyzed the histopathologic changes at 35 dpi in the lungs of BALB/c mice with metastatic mammary tumors that were treated with anti-IL17 or IgG control antibodies. Control antibody-treated mice showed a complete loss of lung architecture and presented numerous colonies of tumor cells and a predominance of polymorphonuclear cells in the lungs. On the contrary, anti–IL17-treated mice exhibited preserved lung architecture, reduced numbers of tumor cells, and polymorphonuclear cells (Fig. 3A). These results were further confirmed by flow-cytometry analysis of lung-extracted leukocytes, which showed a significant reduction in the number of neutrophils in the lungs of anti–IL17-treated mice compared with those of control antibody-treated mice (Fig. 3B). We then evaluated the expression of the protumorigenic neutrophil markers TNFα and MMP-9. As expected, the number of TNFα-producing $CD11b^{+}Ly6G^{+}$ neutrophils was significantly elevated in the lungs of animals with a mammary tumor and treated with a control antibody, but was massively reduced in the lungs of anti–IL17A-treated mice (Fig. 3C). qPCR analysis of total lung tissue showed a significant reduction in the relative expression of MMP-9 in animals treated with anti-IL17 in comparison with those treated with control antibody (Fig. 3D). On the other hand, the expression of IFNγ was similar in both groups (Supplementary Fig. S2). Together, these results indicate that IL17 participates in tumor progression, possibly by recruiting neutrophils to secondary sites affected by the tumor, thus favoring disease progression.

Protumorigenic neutrophils control tumor growth in metastatic mammary tumors

The findings reported above led us to assess the contribution of neutrophils to disease progression in our tumor model. We first analyzed the numbers of neutrophils in the spleens of metastatic and nonmetastatic tumor-bearing mice. The numbers of $Ly6G^{+}F4/80^{-}$ neutrophils ($CD11b^{+}MHCII^{-}$) were significantly increased in 4T-1 tumor-bearing mice in comparison with 67NR tumor-bearing hosts and naïve mice (Fig. 4A). Furthermore, we found high numbers of tumor-infiltrating neutrophils at 25 and 35 dpi within the 4T-1 tumors, as assessed by flow cytometry (Fig. 4B) and histologic analysis (Fig. 4C). In line with the finding that protumorigenic neutrophil contributes to angiogenesis, invasion, metastasis, and immunosuppression (18), we also found that neutrophils isolated from the spleens and tumors of 4T-1 tumor-bearing mice presented a high expression of genes related to protumorigenic neutrophils, including *Cxcl1*, *Tnf-α*, *Mmp-9*, and *Vegf* (Fig. 4D). To further test the role of tumor-associated neutrophils, we treated BALB/c mice undergoing metastatic tumor (4T-1) induction with anti–Ly6G-neutralizing antibody and analyzed tumor progression. The depletion of neutrophils *in vivo* did not alter an IL17A production in the tumor (Supplementary Fig. S3A and S3B); however, promoted a significant reduction of the

volume (Fig. 4E and F) and weight of the tumor mass (Fig. 4G) in tumor-bearing mice. Thus, the recruitment of protumorigenic neutrophils contributes to tumor progression.

IL17A induces the production of IL6 and CCL20 in murine metastatic mammary carcinoma cells

To determine the effects of IL17A on tumor cells, the 4T-1 and 67NR cells lines were cultured for 48 hours in the presence or absence of recombinant IL17A (rIL17). The 4T-1 cells exhibited high CCL20 production that was increased with IL17 treatment (Fig. 5B). However, we found a low level of IL6 expression in the 4T-1 cells, which was increased with IL17 treatment (Fig. 5A and B). Therefore, IL6 production is dependent IL17 on 4T-1 cells. By contrast, nonmetastatic 67NR cells demonstrated low expression of IL6 and CCL20 independent of IL17 treatment (Fig. 5A and B). Thus, metastatic and nonmetastatic tumor cells display different responses to IL17A *in vitro*.

IL6 is required for Th17 differentiation and is involved in the inflammation associated with tumorigenesis (19, 20). To test the relevance of IL6 in tumor progression and its contribution to the responses of Th17 cells. BALB/c mice undergoing 4T-1 tumor induction were treated with anti–IL6-neutralizing antibody, and tumor progression was evaluated. The depletion of IL6 *in vivo* significantly lowered the tumor volume in comparison with control mice (treated with IgG control; Fig. 5C). In addition, our data showed a decrease in the numbers of $CD4^+IL17A^+$ T cells (Fig. 5D) and neutrophils ($Ly6G^+F4/80^-$) gated on $CD11b^{hi}MHCII^-$ cells in the spleens of animals treated with anti-IL6 (Fig. 5E) compared with the control group. Similarly, we found a reduction of IL17A (Supplementary Fig. S3A and S3D) and polymorphonuclear cells (Fig. 5F) in tumor of mice treated with anti-IL6 mAb compared with the controls.

To further evaluate whether the Th17 response in the tumor is dependent on factors produced by metastatic tumor cells *in vivo*, we generated an air pouch in the dorsal side of BALB/c mice and locally injected 4T-1 and 67NR cell supernatant, CCL20 as an inflammatory stimulus or PBS as a control. Twenty hours later, we found that the numbers of IL17-producing $CD3^+$ cells recruited into the air pouch were significantly higher in the 4T-1 supernatant-treated group than in the PBS control group and comparable with the CCL20-treated mice (Fig. 5G). In response to the 67NR supernatant, we observed that similar numbers of $IL17^+CD3^+$ cells were recruited into the air pouch compared with the control group (treated with PBS). Therefore, the 4T-1 cell supernatants induce the migration of preexisting T cells producing IL17. IL17 promotes the production of IL6 and CCL20 initiates a feedback loop to foster the amplification of the Th17 response.

IL17A directly affects nonmetastatic mammary tumor cell behavior *in vivo*

To assess whether IL17 affects the growth of nonmetastatic primary tumor, we pretreated 67NR cells with rIL17 before injecting them into BALB/c mice and analyzed the tumor progression. The IL17-pretreated 67NR cells promoted a significantly increased tumor volume compared with that of mice injected with untreated 67NR cells and comparable with that of 4T-1 tumor-bearing mice (Fig. 6A). Moreover, the number of neutrophils in the spleens (Fig. 6B) and tumor (Fig. 6C) of mice inoculated with IL17-pretreated 67NR cells

was increased compared with those that received untreated 67NR cells, and it was similar to that of 4T-1 tumor-bearing mice (Fig. 6B).

To understand how IL17 induces an increase in nonmetastatic tumor growth, we analyzed the gene-expression profile of the 67NR cells lines that were either treated or not treated with IL17A, using a microarray analysis. Strikingly, using a threshold of at least 2-fold, we identified 1,742 upregulated and 2,592 downregulated genes in the IL17-treated cells compared with the untreated cells (Fig. 6D). In addition, we found an increased expression of genes related to cellular adhesion (*Itga1*, *Itgb1*, *Itgb3*, *Cadm4*, *Icam1*, *Spam1*, *Ceacam13*, and *Ceacam19*); cellular growth and survival (*Cdc20b*, *Cdc25b*, *Erg1*, *Egfr*, *Ciapin1*, *Bcl2l14*, and *Il24*); chemokine and chemokine receptors (*Ccr1*, *Ccr2*, *Cxcr2*, *Cxcr3*, *Cxcr4*, *Cxcr5*, *Ccl3*, *Cxcl2*, and *Cxcl11*); and cytokines, receptors and molecules associated with angiogenesis and metastasis (*Tgfb1i1*, *Il1a*, *Il18r1*, *Il18rap*, *Tnfsf12*, *Ptger3*, *Pdcd11*, *Hmox1*, *Twist1*, and *Vegfa*; (Fig.6D). A complete list of the differentially expressed genes is presented in Supplementary Tables S2 and S3.

To confirm whether IL17 actually promotes more aggressive tumor cells, we compared the gene-expression profile of 4T-1 cells with IL17-treated 67NR cells. Interestingly, we found 279 upregulated genes in common between the IL17-treated 67NR cells and 4T-1 cells compared with the untreated 67NR cells (Fig.6E). Among the differentially expressed genes, we identified *Itga1*, *Icam-1*, *Egfr*, *Cxcr3*, *Cxcr4*, *Ccl3*, *Il1a*, *LTb4r2*, and *Twist1* related to the cellular adhesion, growth, and migration of tumor cells. Taken together, these results indicate that IL17 has a direct effect on tumor cells, altering the gene-expression profile and making the cells more aggressive, favoring tumor growth *in vivo*.

IL17A expression predicts clinical outcome in human invasive breast cancer

The results described above, along with our recent observation that the presence of IL17-producing T cells in the tumoral microenvironment is associated with disease progression in patients with breast cancer (16), led us to inquire whether the tumor microenvironment of patients with IDC could, in fact, promote Th17 differentiation. We first assessed whether cytokines that drive Th17 differentiation could be promptly measured in such tumors. A qPCR analysis revealed that the expression of IL6 ($P = 0.003$) and CCL20 ($P = 0.003$) mRNA was significantly increased in breast tumor tissue when compared with control tissue (Fig. 7A). Interestingly, IL6 expression was upregulated in $IL17^{hi}$ human breast tumor samples; however, the expression of CCL20 was similar in $IL17^{hi}$ and $IL17^{lo}$ samples (Supplementary Fig. S4). An immunohistochemistry analysis confirmed that IL6 and CCL20 protein were selectively expressed in tumor tissues but not in control–tissue biopsies (Fig. 7B). These data indicate that invasive human breast tumors provide a favorable environment for the development, maintenance and migration of Th17 cells.

To further investigate how IL17 production could directly affect the biology of tumors in humans, we grouped breast tumor samples according to their expression of IL17A, and then compared their gene-expression profiles using microarray analysis. Strikingly, principal component analysis revealed that low and high IL17 producers showed distinct global gene-expression profiles (Fig. 7C). Using a threshold of at least 2-fold and a *P* value of <0.01, we identified 74 upregulated (red) and 168 downregulated (blue) genes in tumor samples from

patients with IL17^{hi} in comparison with IL17^{lo} tumors (Fig. 7C and D, Supplementary Tables S4 and S5). In addition, a substantial proportion of the differentially expressed genes in these samples were related to tumor progression, and their expression was confirmed by qPCR (Supplementary Fig. S4). Genes that were upregulated in IL17^{hi} tumor samples included *USP28*, a ubiquitin-specific protease involved in the proliferation of tumor cells (21), *BCL-2* (B-cell lymphoma 2), a dominant repressor of cell death that promotes cell survival (22), and *FAIM* (Fas apoptosis inhibitory molecule), an antiapoptotic molecule (21). By contrast, the expression of *GAS-7* (growth arrest-specific protein 7), a gene related to cell growth/arrest (22), was reduced compared with the IL17^{lo} tumor samples.

To further investigate the clinical significance of IL17A in human breast cancer, the clinicopathologic factors of breast cancer, such as tumor size, lymph node status (positive and negative axilla), and the survival of patients, were analyzed relative to the intratumoral expression of IL17A. The clinical characteristics of the patients studied are reported in Supplementary Table S5. Interestingly, we found that 75% of the patients with IL17^{hi} expression exhibited tumors larger than 5 cm (T3); 92% of these patients were lymph node positive, and 42% showed recurrent disease. In contrast, 64% of patients with IL17^{lo} expression presented tumors up to 5 cm and were classified as T2, 73% of them presented negative axilla, and 100% of the patients showed no recurrence of disease (Supplementary Table S6). In contrast, patients with low expression of IL17A demonstrated improved DFS rates compared with patients with high expression of this gene (Fig. 7E; $P = 0.047$). Together, the results indicate that IL17A promotes the development of aggressive tumors through mechanisms involving direct effects on tumor cells and the immune system.

Discussion

In this study, we uncovered the mechanism by which the proinflammatory cytokine IL17A promotes metastatic mammary primary tumor progression. We showed that the presence of IL17A in tumor tissues isolated from IDC patients correlates with poor prognosis and a high expression of genes that promote the proliferation and survival of these tumors. Confirming the data from humans, in our murine mammary tumor model, IL17 changes the behavior of nonmetastatic cells, promoting tumor growth. Thus, we propose that inhibition of IL17 could have broad clinical applications in invasive breast cancer. Recently, we demonstrated that the enrichment of Treg cells in IDC patients correlates with upregulation of IL17A expression and invasiveness of the tumor (16). Consistent with these findings, tumor-infiltrating Th17 cells were shown to correlate with worse prognosis in patients with colorectal and lung cancer (10, 23). Despite the potential therapeutic implications of these observations, especially in the context of the link between inflammation and tumor growth, the mechanisms underlying the modulation of tumor progression by IL17 are not yet known.

To study the role of IL17 in tumor progression, we took advantage of the previously established 4T-1 metastatic breast cancer model in BALB/c mice, which is an excellent model for studying the progression of breast cancer in humans. This model has been used to study antitumor immune mechanisms that counteract tumor growth and metastasis (17). Using this model, we showed that IL17A is produced in the metastatic primary tumor microenvironment by CD3$^+$CD4$^+$ and CD3$^+\gamma\delta^+$ T cells. And IL17 blockade significantly

inhibited tumor growth, indicating the role of IL17 in mammary tumor growth. In TC-1 tumor model, we also showed that the TILs produce IL17A, and that its blockage reduces the volume tumor. Another models as B16 melanoma, tumor growth was inhibited in $IL17^{-/-}$ mice and in IFNγ/IL17 double-knockout mice (24). On the contrary, in the ovarian carcinoma model, tumor growth was increased in $IL17^{-/-}$ mice because the absence of IL17 caused decreased numbers of IFNγ-producing natural killer and T cells (25). Although it was suggested that IFNγ plays a role in the regulation of antitumor immune responses (26), our results indicate that IFNγ does not play a direct role in controlling tumor development in the 4T1 model. In addition, and in contrast with IL17, the IFNγ production was neither altered with the disease progression nor when IL17 was blocked. However, we cannot exclude the possibility of an indirect role of IFNγ in this process via regulation of IL17 production (27–29). Thus, it is conceivable that the downstream effects of the IL17 blockade in regulating tumor growth is tumor model specific.

The mechanism by which IL17 promotes the growth of metastatic primary mammary tumors is neutrophil dependent. Once the IL17 blockade-induced reduction in mammary tumor size was accompanied by decreased numbers of neutrophils in the tumor microenvironment and tumor cell colonies at secondary sites of tumor formation. This beneficial effect of anti-IL17A antibody therapy was also associated with decreased MMP-9 expression and reduced numbers of TNFα-producing neutrophils, indicating that the main role of IL17 in this model is to promote the recruitment of protumorigenic neutrophils. Tumor-associated neutrophils differentiate in response to tumor-produced factors, such as TGFβ, that is produced by tumor and inflammatory cells (14) and contribute to angiogenesis, metastasis, and immunosuppression in tumor-bearing hosts (30).

In a lung cancer model, it has been shown that neutrophils invading the lungs exert protumorigenic activity through the release of MMP-9, which favors the survival and establishment of tumor cells (31). Furthermore, neutrophils also promote the release of proinflammatory factors, such as TNFα, in a melanoma model (32) and human tumors, including hepatocellular and cervical carcinomas (33), which, in turn, favor angiogenesis and metastasis. To facilitate invasion, neutrophils might directly degrade the extracellular matrix via the release of several enzymes, such as neutrophil elastase, cathepsin G, proteinase-3, MMP-8, and MMP-9 (34). In our studies, neutrophils isolated from tumor sites and the spleen produced high levels of CXCL1, TNFα, MMP-9, and VEGF, all of which are associated with disease progression (35). In line with this finding, despite the depletion of neutrophils *in vivo* did not change the IL17A production into the tumor, it promoted an inhibition of 4T-1 tumor growth, confirming the protumorigenic role of neutrophils in this model.

In addition to the recruitment of neutrophils, IL17 also induces IL6 and CCL20 production in metastatic tumor cells, which in turn promote the recruitment and differentiation of Th17 cells. The initial recruitment of IL17-producing T cells creates a feed-forward loop that sustains the inflammatory environment at the tumor site with high production of IL6 and CCL20, maintaining the profile of the Th17 response. Indeed, the depletion of IL6 *in vivo* promotes the inhibition of tumor growth and decreases the Th17 response and neutrophil migration, suggesting that IL17-mediated tumor progression is dependent on IL6.

Regardless, CCL20 is an essential factor affecting the prevalence of the Th17 response in a tumor. Interestingly, the direct effects of IL17 in inducing the production of inflammatory cytokines were specific to metastatic (4T-1) tumor cells, as the nonmetastatic tumor cell line (67NR) was refractory to the effects of IL17, although both tumor cell lines expressed the receptor for IL17. Nonetheless, these results explain why the Th17 response is increased in metastatic tumor-bearing mice compared with nonmetastatic tumor-bearing mice.

In line with this finding, tumor tissues from patients with IDC showed higher expression of IL6 and CCL20, which would also provide a favorable environment for the migration and maintenance of Th17 cells. On the basis of these observations and the previously established tight association between TGFβ and IL6 with tumor incidence and progression in patients with cancer, it appears likely that $CD4^+$ T cells entering an established tumor are more likely to be exposed to conditions that induce the differentiation of Th17 compared with other Th subsets (20, 36, 37). Thus, the feed-forward loop we are describing for the murine 4T1 models might very well be present in human breast tumors.

Interestingly, the presence of IL17 in patients with IDC was associated with a worse prognosis and a high expression of genes related to the proliferation and survival of these tumors. This effect occurs because IL17 determines the aggressiveness of the tumor cells. IL17 is able to change the behavior of nonmetastatic 67NR cells, inducing the expression of various genes associated with the cellular adhesion, proliferation, and migration of tumor cells. For example, breast tumor cells with high ICAM-1 (38), CXCR3 (39), and Twist (40) expression exhibit metastatic potential. These alterations generated in 67NR cells after treatment with IL17 induced increased tumor growth and levels of neutrophils; this finding might explain why IL17 induces increased expression of mediators such as CXCL11 and Ltb4r2 (leukotriene B4 receptor 2) in 67NR tumor cells, which are genes related to neutrophil chemotaxis (41).

Taken together, our data support a model in which preexisting T cells producing IL17 are recruited to the tumor site promote an inflammatory environment with a high IL6 and CCL20 production that promotes their own differentiation in addition to promoting the recruitment of protumorigenic neutrophils. Once at the tumor site, tumor-associated neutrophils secrete mediators, such as MMP-9, VEGF, TNFα, and CXCL1, which together promote tumor invasion and metastasis to secondary sites such as the lung. Notably, the induced tumor cell trigger determines the response profile that will be formed in the tumor microenvironment. The presence of IL17 is crucial for disease aggressiveness. Therefore, our results support the idea that IL17, and perhaps expression of the IL17 receptor, in tumor cells could serve as a biomarker for the prognosis of aggressive breast cancer. Further studies will be needed to determine whether these findings can be generalized to other types of invasive tumors. Nonetheless, our findings illustrate the therapeutic potential of IL17 inhibition for specific breast cancer types, which represents an attractive approach for the treatment of invasive breast tumors.

Supplementary Material

Refer to Web version on PubMed Central for supplementary material.

Acknowledgments

The authors are grateful to Cristiane Milanezi and Wander Cosme (FMRP-USP) and to Vincent Funari and Jordan Brown (CSMC) for their technical assistance.

The authors are grateful to Cristiane Milanezi and Wander Cosme (FMRP-USP) and to Vincent Funari and Jordan Brown (CSMC) for their technical assistance.

This work was supported by a Fundação de Amparo a Pesquisa do Estado de São Paulo grant 2012/14524-9, 2013/08216-2, 2012/08240-8 (a scholarship to L. Benevides), NIH-NIAID grant AI083948-01, and by funds from the IBIRI (G.A. Martins).

The costs of publication of this article were defrayed in part by the payment of page charges. This article must therefore be hereby marked *advertisement* in accordance with 18 U.S.C. Section 1734 solely to indicate this fact.

This work was supported by a Fundação de Amparo a Pesquisa do Estado de São Paulo grant 2012/14524-9, 2013/08216-2, 2012/08240-8 (a scholarship to L. Benevides), NIH-NIAID grant AI083948-01, and by funds from the IBIRI (G.A. Martins).

The costs of publication of this article were defrayed in part by the payment of page charges. This article must therefore be hereby marked *advertisement* in accordance with 18 U.S.C. Section 1734 solely to indicate this fact.

References

1. Ferlay J, Parkin DM, and Steliarova-Foucher E, Estimates of cancer incidence and mortality in Europe in 2008. Eur J Cancer, 2010. 46(4): p. 765–81. [PubMed: 20116997]
2. Schmitt CA, Senescence, apoptosis and therapy--cutting the lifelines of cancer. Nat Rev Cancer, 2003. 3(4): p. 286–95. [PubMed: 12671667]
3. Tlsty TD and Coussens LM, Tumor stroma and regulation of cancer development. Annu Rev Pathol, 2006. 1: p. 119–50. [PubMed: 18039110]
4. Pierce BL, et al., Elevated biomarkers of inflammation are associated with reduced survival among breast cancer patients. J Clin Oncol, 2009. 27(21): p. 3437–44. [PubMed: 19470939]
5. Chen Z, Laurence A, and O'Shea JJ, Signal transduction pathways and transcriptional regulation in the control of Th17 differentiation. Semin Immunol, 2007. 19(6): p. 400–8. [PubMed: 18166487]
6. da Matta Guedes PM, et al., IL-17 produced during Trypanosoma cruzi infection plays a central role in regulating parasite-induced myocarditis. PLoS Negl Trop Dis, 2010. 4(2): p. e604 [PubMed: 20169058]
7. Khader SA, et al., IL-23 and IL-17 in the establishment of protective pulmonary CD4+ T cell responses after vaccination and during Mycobacterium tuberculosis challenge. Nat Immunol, 2007. 8(4): p. 369–77. [PubMed: 17351619]
8. Steiner GE, et al., Expression and function of pro-inflammatory interleukin IL-17 and IL-17 receptor in normal, benign hyperplastic, and malignant prostate. Prostate, 2003. 56(3): p. 171–82. [PubMed: 12772186]
9. Zhang B, et al., The prevalence of Th17 cells in patients with gastric cancer. Biochem Biophys Res Commun, 2008. 374(3): p. 533–7. [PubMed: 18655770]
10. Reppert S, et al., A role for T-bet-mediated tumour immune surveillance in anti-IL-17A treatment of lung cancer. Nat Commun, 2011. 2: p. 600. [PubMed: 22186896]
11. Ciree A, et al., Expression and activity of IL-17 in cutaneous T-cell lymphomas (mycosis fungoides and Sezary syndrome). Int J Cancer, 2004. 112(1): p. 113–20. [PubMed: 15305382]
12. Grivennikov SI, Wang K, Mucida D, Stewart CA, Schnabl B, Jauch D, et al. Adenoma-linked barrier defects and microbial products drive IL-23/IL-17-mediated tumour growth. Nature 2012;491:254–8 [PubMed: 23034650]
13. Wu S, et al., A human colonic commensal promotes colon tumorigenesis via activation of T helper type 17 T cell responses. Nat Med, 2009. 15(9): p. 1016–22. [PubMed: 19701202]
14. Fridman WH, et al., The immune microenvironment of human tumors: general significance and clinical impact. Cancer Microenviron, 2013. 6(2): p. 117–22. [PubMed: 23108700]

15. Park H, et al., A distinct lineage of CD4 T cells regulates tissue inflammation by producing interleukin 17. Nat Immunol, 2005. 6(11): p. 1133–41. [PubMed: 16200068]
16. Benevides L, et al., Enrichment of regulatory T cells in invasive breast tumor correlates with the upregulation of IL-17A expression and invasiveness of the tumor. Eur J Immunol, 2013. 43(6): p. 1518–28. [PubMed: 23529839]
17. Tao K, et al., Imagable 4T1 model for the study of late stage breast cancer. BMC Cancer, 2008. 8: p. 228 [PubMed: 18691423]
18. Fridlender ZG and Albelda SM, Tumor-associated neutrophils: friend or foe? Carcinogenesis, 2012. 33(5): p. 949–55. [PubMed: 22425643]
19. Veldhoen M, et al., TGFbeta in the context of an inflammatory cytokine milieu supports de novo differentiation of IL-17-producing T cells. Immunity, 2006. 24(2): p. 179–89. [PubMed: 16473830]
20. Yao X, et al., Targeting interleukin-6 in inflammatory autoimmune diseases and cancers. Pharmacol Ther, 2014. 141(2): p. 125–39. [PubMed: 24076269]
21. Oster SK, et al., The myc oncogene: MarvelouslY Complex. Adv Cancer Res, 2002. 84: p. 81–154. [PubMed: 11885563]
22. Strasser A, Huang DC, and Vaux DL, The role of the bcl-2/ced-9 gene family in cancer and general implications of defects in cell death control for tumourigenesis and resistance to chemotherapy. Biochim Biophys Acta, 1997. 1333(2): p. F151–78. [PubMed: 9395285]
23. Tosolini M, et al., Clinical impact of different classes of infiltrating T cytotoxic and helper cells (Th1, th2, treg, th17) in patients with colorectal cancer. Cancer Res, 2011. 71(4): p. 1263–71. [PubMed: 21303976]
24. Wang L, et al., IL-17 can promote tumor growth through an IL-6-Stat3 signaling pathway. J Exp Med, 2009. 206(7): p. 1457–64. [PubMed: 19564351]
25. Kryczek I, et al., Endogenous IL-17 contributes to reduced tumor growth and metastasis. Blood, 2009. 114(2): p. 357–9. [PubMed: 19289853]
26. Dunn GP, Koebel CM, and Schreiber RD, Interferons, immunity and cancer immunoediting. Nat Rev Immunol, 2006. 6(11): p. 836–48. [PubMed: 17063185]
27. Gocke AR, Cravens PD, Ben LH, Hussain RZ, Northrop SC, Racke MK, et al..T-bet regulates the fate of Th1 and Th17 lymphocytes in autoimmunity. J Immunol 2007;178:1341–8. [PubMed: 17237380]
28. Mathur AN, Chang HC, Zisoulis DG, Kapur R, Belladonna ML, Kansas GS, et al. T-bet is a critical determinant in the instability of the IL-17-secreting T-helper phenotype. Blood 2006;108:1595–601. [PubMed: 16670261]
29. Guo S, Cobb D, Smeltz RB. T-bet inhibits the *in vivo* differentiation of parasite-specific $CD4^+$ Th17 cells in a T cell-intrinsic manner. J Immunol 2009;182:6179–86. [PubMed: 19414771]
30. Fridlender ZG, et al., Polarization of tumor-associated neutrophil phenotype by TGF-beta: “N1” versus “N2” TAN. Cancer Cell, 2009. 16(3): p. 183–94. [PubMed: 19732719]
31. Acuff HB, et al., Matrix metalloproteinase-9 from bone marrow-derived cells contributes to survival but not growth of tumor cells in the lung microenvironment. Cancer Res, 2006. 66(1): p. 259–66. [PubMed: 16397239]
32. Bald T, Quast T, Landsberg J, Rogava M, Glodde N, Lopez-Ramos D, et al. Ultraviolet-radiation-induced inflammation promotes angiotropism and metastasis in melanoma. Nature 2014;507:109–13. [PubMed: 24572365]
33. Wu Y, Zhao Q, Peng C, Sun L, Li XF, Kuang DM. Neutrophils promote motility of cancer cells via a hyaluronan-mediated TLR4/PI3K activation loop. J Pathol 2011;225:438–47 [PubMed: 21826665]
34. Dumitru CA, Lang S, and Brandau S, Modulation of neutrophil granulocytes in the tumor microenvironment: mechanisms and consequences for tumor progression. Semin Cancer Biol, 2013. 23(3): p. 141–8. [PubMed: 23485549]
35. Nozawa H, Chiu C, and Hanahan D, Infiltrating neutrophils mediate the initial angiogenic switch in a mouse model of multistage carcinogenesis. Proc Natl Acad Sci U S A, 2006. 103(33): p. 12493–8. [PubMed: 16891410]

36. Flavell RA, Sanjabi S, Wrzesinski SH, Licona-Limon P. The polarization of immune cells in the tumour environment by TGFbeta. Nat Rev Immunol 2010;10:554–67 [PubMed: 20616810]

37. Salgado R, Junius S, Benoy I, Van Dam P, Vermeulen P, Van Marck E,et al. Circulating interleukin-6 predicts survival in patients with metastatic breast cancer. Int J Cancer 2003;103:642–6. [PubMed: 12494472]

38. Rosette C, Roth RB, Oeth P, Braun A, Kammerer S, Ekblom J, et al. Role of ICAM1 in invasion of human breast cancer cells. Carcinogenesis 2005;26:943–50. [PubMed: 15774488]

39. Kawada K, Hosogi H, Sonoshita M, Sakashita H, Manabe T, Shimahara Y, et al. Chemokine receptor CXCR3 promotes colon cancer metastasis to lymph nodes. Oncogene 2007;26:4679–88. [PubMed: 17297455]

40. Yang J, Mani SA, Donaher JL, Ramaswamy S, Itzykson RA, Come C, et al. Twist, a master regulator of morphogenesis, plays an essential role in tumor metastasis. Cell 2004;117:927–39. [PubMed: 15210113]

41. Ford-Hutchinson AW, Bray MA, Doig MV, Shipley ME, Smith MJ. Leukotriene B, a potent chemokinetic and aggregating substance released from polymorphonuclear leukocytes. Nature 1980;286:264–5. [PubMed: 6250050]

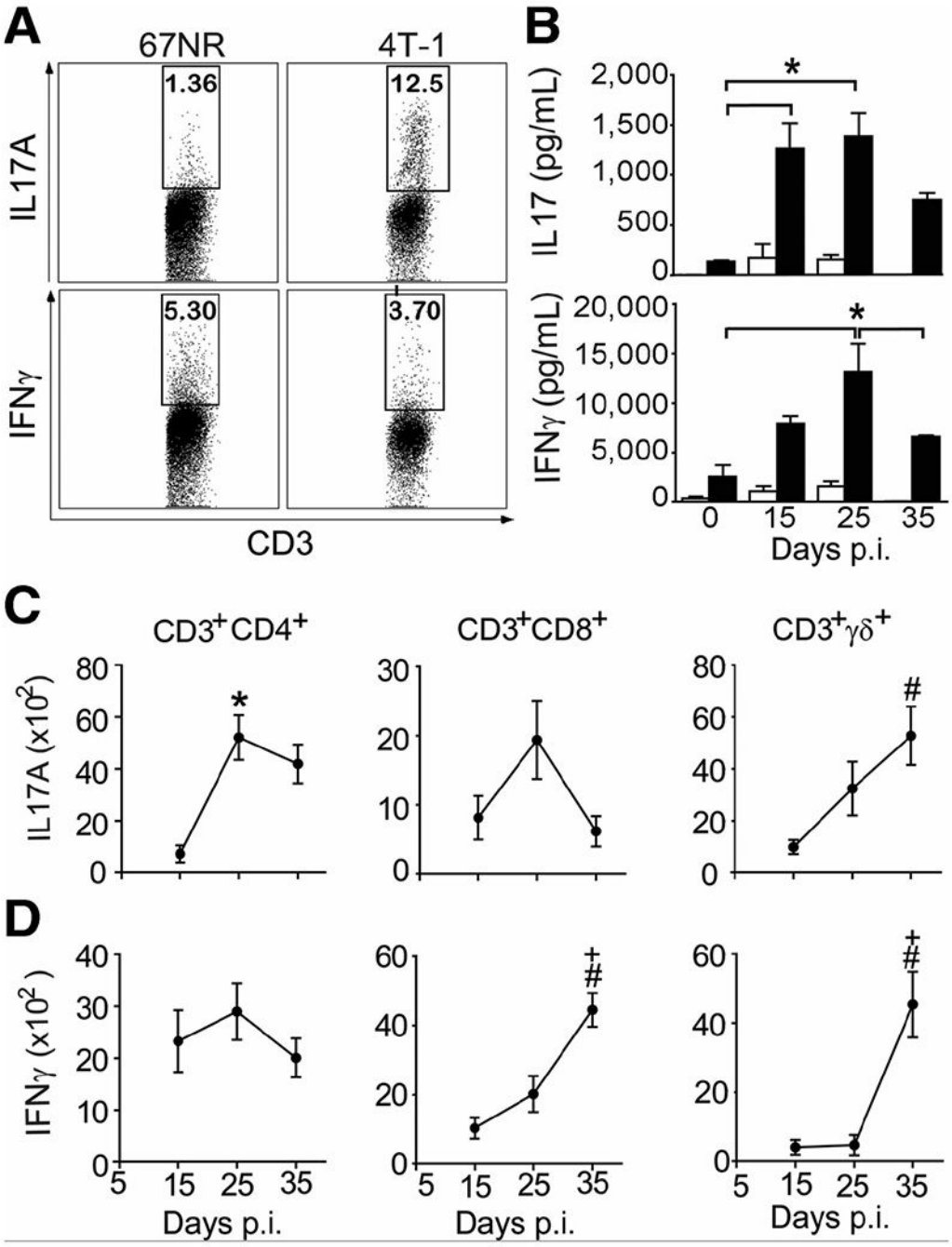

Figure 1. IL17A is produced in murine metastatic mammary tumors.

A, cytokine production by tumor-infiltrating cells isolated from BALB/c mice subjected to an induction protocol with nonmetastatic (67NR) and metastatic (4T-1) mammary tumors on day 15 postinoculation (p.i.). Cells were stimulated with PMA + ionomycin, and the expression of IL17A and IFNγ was analyzed in $CD3^+$ cells using flow cytometry. B, IL17A and IFNγ levels (measured by ELISA) in the supernatants of splenocytes isolated at day 0, 15, 25, and 35 postinoculation with 4T-1 and stimulated with anti-CD3 + anti-CD28 (closed bars) or unstimulated (open bars) for 72 hours. C and D, total numbers of PMA/ionomycin-

stimulated, CD3-gated, $CD4^+$, $CD8^+$, and $TCR\gamma\delta^+$ T cells producing IL17A (C) and IFNγ (D) in isolates from the tumor microenvironment (measured by flow cytometry). The data shown are representative of three independent experiments with similar results and are shown as the mean ± SEM of five mice (*, $P < 0.05$, comparing periods of 15–25 days; +, $P < 0.05$, comparing periods of 25–35 days; #, $P < 0.05$, comparing periods of 15–35 days).

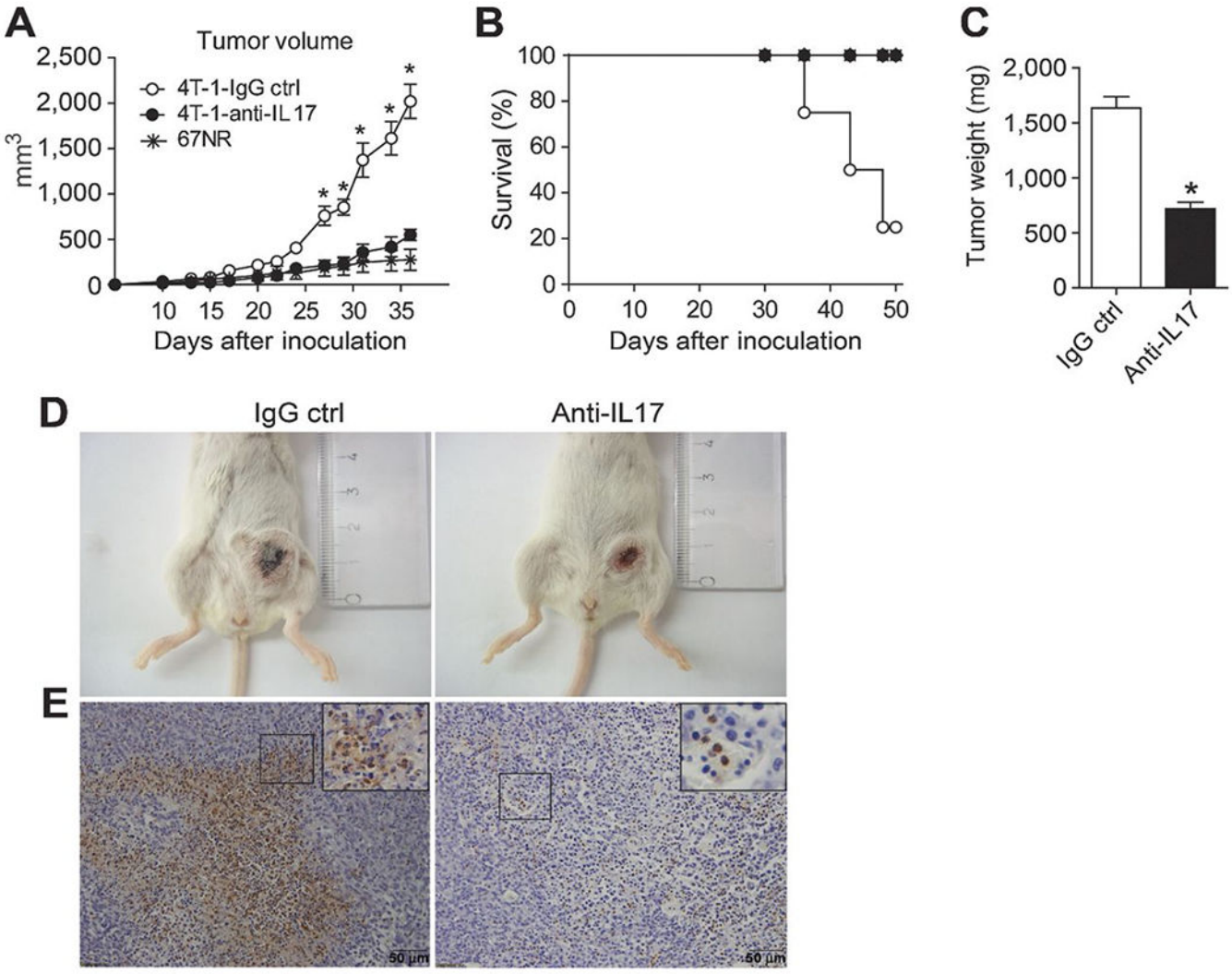

Figure 2. Treatment with anti-IL17 inhibits the growth of murine mammary tumors.

BALB/c mice were subjected to an induction protocol with mammary tumor cells (4T1, squares) or treated with neutralizing anti-IL17A (filled squares) or rat immunoglobulin (IgG control; open squares) antibodies or 67NR (asterisks). A, the volume of the tumors was measured at 10 dpi. B, the percentage of survival was assessed daily. C, at 35 dpi, the weight of the tumors was measured. The data shown are representative of two independent experiments with similar results and are shown as the mean ± SEM of five mice per group (*, $P < 0.05$). D, photographs show representative tumors in mice treated with the IgG control (left) or anti-IL17 antibodies (right) at 35 dpi. E, immunohistochemical staining in tumor tissue of the mice treated with the IgG control (left) or anti-IL17 mAb (right) at 35 dpi was used to detect Ly6G protein; scale bars, 50 µm.

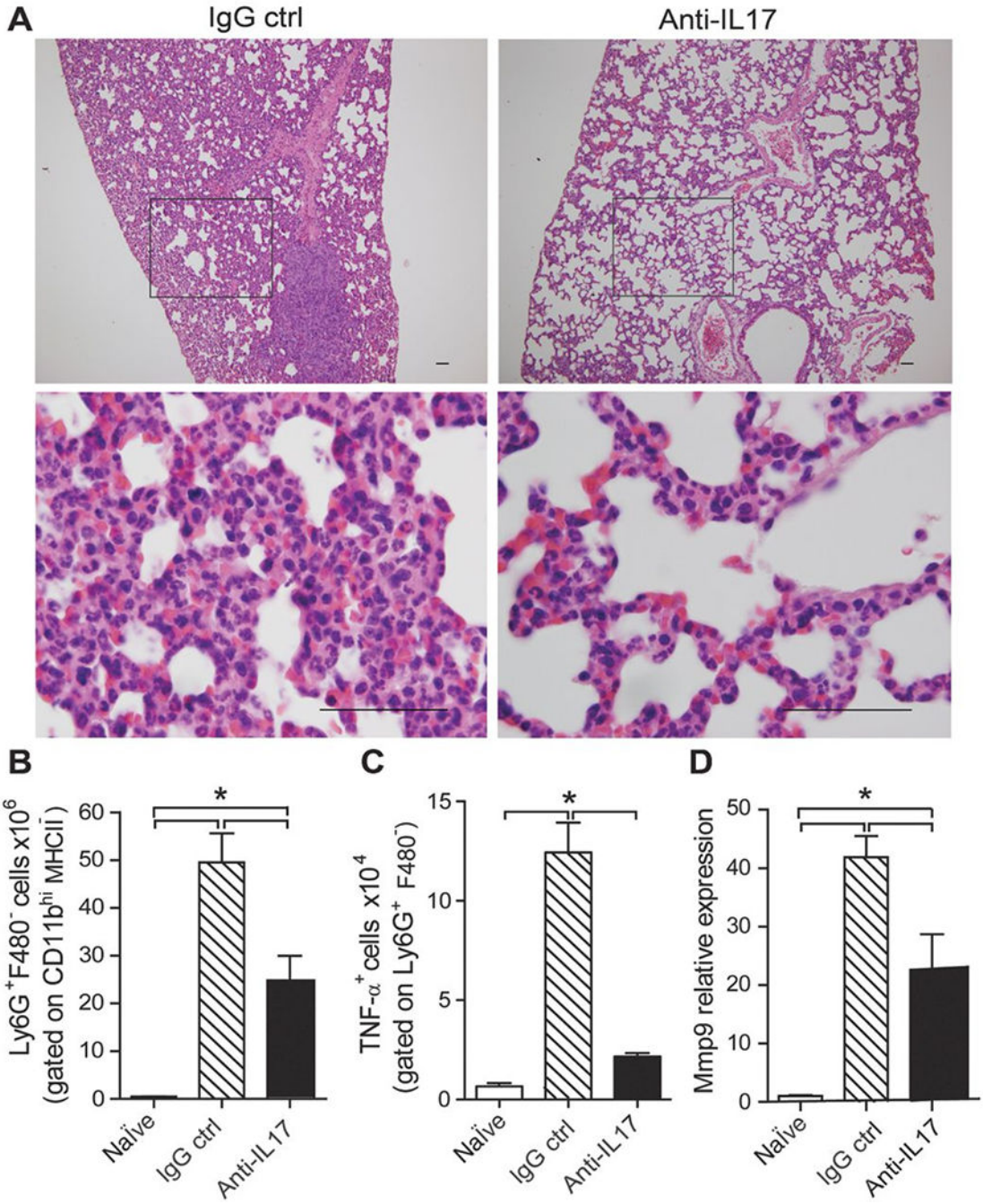

Figure 3. Blockade of IL17 inhibits neutrophil recruitment to the lung in a metastatic mammary tumor model.

BALB/c mice were subjected to an induction protocol with mammary tumors and treated with anti-IL17A or IgG control antibodies. A, representative H&E-stained sections of lung tissue collected at 35 dpi; original magnification, ×10 (top) and ×100 (bottom); scale bars, 50 μm. B and C, flow cytometric analysis of the numbers of neutrophils ($Ly6G^+F4/80^-$) gated on $CD11b^+MHCII^-$ cells (B) and $TNF\alpha^+$ cells gated on $Ly6G^+MHCII^-$ cells (C) after isolation from the lung and stimulation with 100 μg/mL of LPS for 6 hours. D, mRNA was isolated from fragments of lung tissue from both groups at 35 dpi, and the relative

expression of MMP-9 was evaluated by qPCR. The data shown are representative of two independent experiments with similar results and are shown as the mean ± SEM of five mice per group (*, $P < 0.05$).

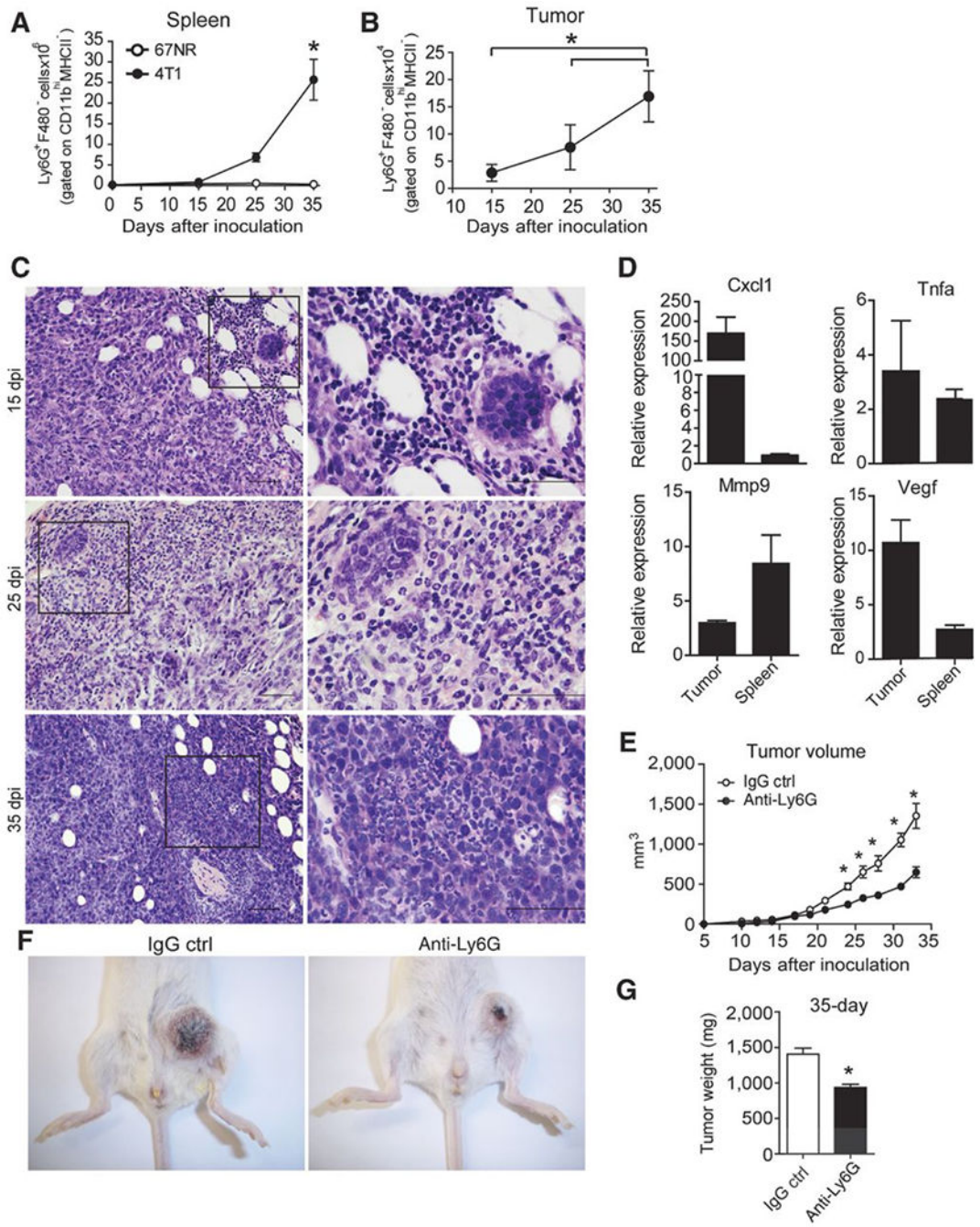

Figure 4. Increased numbers of neutrophils and expression of genes related to the tumorigenic neutrophils phenotype in metastatic murine mammary tumors.

BALB/c mice subjected to an induction protocol with nonmetastatic (67NR) and metastatic (4T-1) mammary tumor cells at day 0, 15, 25, and 35 dpi. The numbers of neutrophils (Ly6G $^{+}$F480^{-}) gated on CD11b^{+}MHCII^{-} cells were analyzed in the population of granulocytes isolated from the spleens (A) and tumors (B) by flow cytometry. C, representative, H&E-stained sections of the tumor microenvironment collected at 15, 25, and 35 dpi; original magnification, ×10 (left) and ×100 (right); scale bars, 50 μm. D, Ly6G^{+}F4/80^{-} cells gated on CD11b^{hi}MHCII^{-} cells were sorted from the spleens and tumors of 4T-1 tumor-bearing mice,

and the expression of MMP-9, VEGF, TNFα, and CXCL1 was analyzed by qPCR. The data shown are normalized to β-actin expression. The data shown represent the means ± SEM compared with $Ly6G^{+}F4/80^{-}$ cells isolated from the spleens of naïve mice. E, the volume of the tumors obtained from BALB/c mice subjected to an induction protocol with mammary tumor cells and treated with anti-Ly6G or rat immunoglobulin (IgG control) antibodies was measured at 10 dpi. F, photographs are representative of tumors in mice treated with IgG control (left) or anti-Ly6G (right) antibodies. G, at 35 dpi, the weight of the tumors was measured. Data are representative of two independent experiments with similar results and are shown as the mean ± SEM of four mice per group (*, $P < 0.05$).

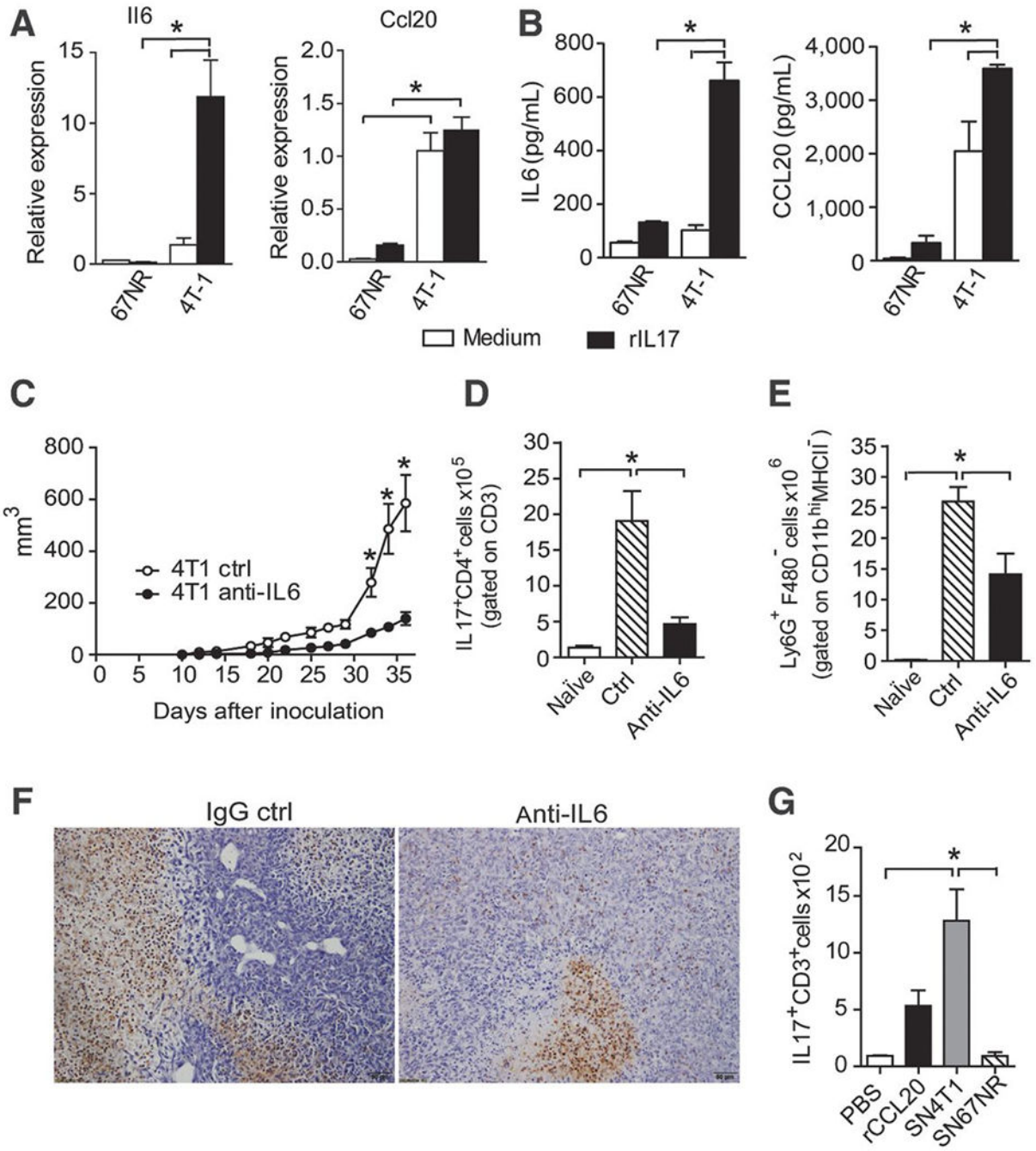

Figure 5. IL17A induces the expression of IL6 and CCL20 in 4T-1 tumor cells lines.

67NR and 4T-1 cells were either treated or not treated with rIL17. After 48 hours, the mRNA was extracted and the culture supernatants were collected. A, the relative expression of IL6 and CCL20 was measured by qPCR. B, the IL6 and CCL20 levels were measured in the culture supernatants by ELISA. The data are representative of two independent experiments with similar results (*, $P < 0.05$). C, the volume of tumors obtained from BALB/c mice subjected to an induction protocol with metastatic (4T-1) mammary tumor cells and treated with anti-IL6 or rat immunoglobulin (IgG control) antibodies was measured

at 10 dpi. At 35 dpi, the numbers of Th17 cells ($IL17^+CD4^+$) gated on $CD3^+$ cells (D) and neutrophils ($Ly6G^+F4/80^-$) gated on $CD11b^+MHCII^-$ cells isolated from the spleen (E) were assessed by flow cytometry. F, immunohistochemical staining in tumor tissues of the mice treated with the IgG control (left) or anti-IL6 mAb (right) at 35 dpi was used to detect Ly6G protein. The data are representative of two independent experiments with similar results and are shown as the mean ± SEM of four mice per group (*, $P < 0.05$). BALB/c mice received PBS, 400 ng of CCL20, and/or a 4T-1 or 67NR supernatant injected into the air pouch, and the cell infiltrates were harvested at 20 hours after injection. G, the total number of IL17A-producing $CD3^+$ cells harvested per pouch was analyzed by flow cytometry. The data are shown as the mean ± SEM of three mice per group (*, $P < 0.05$).

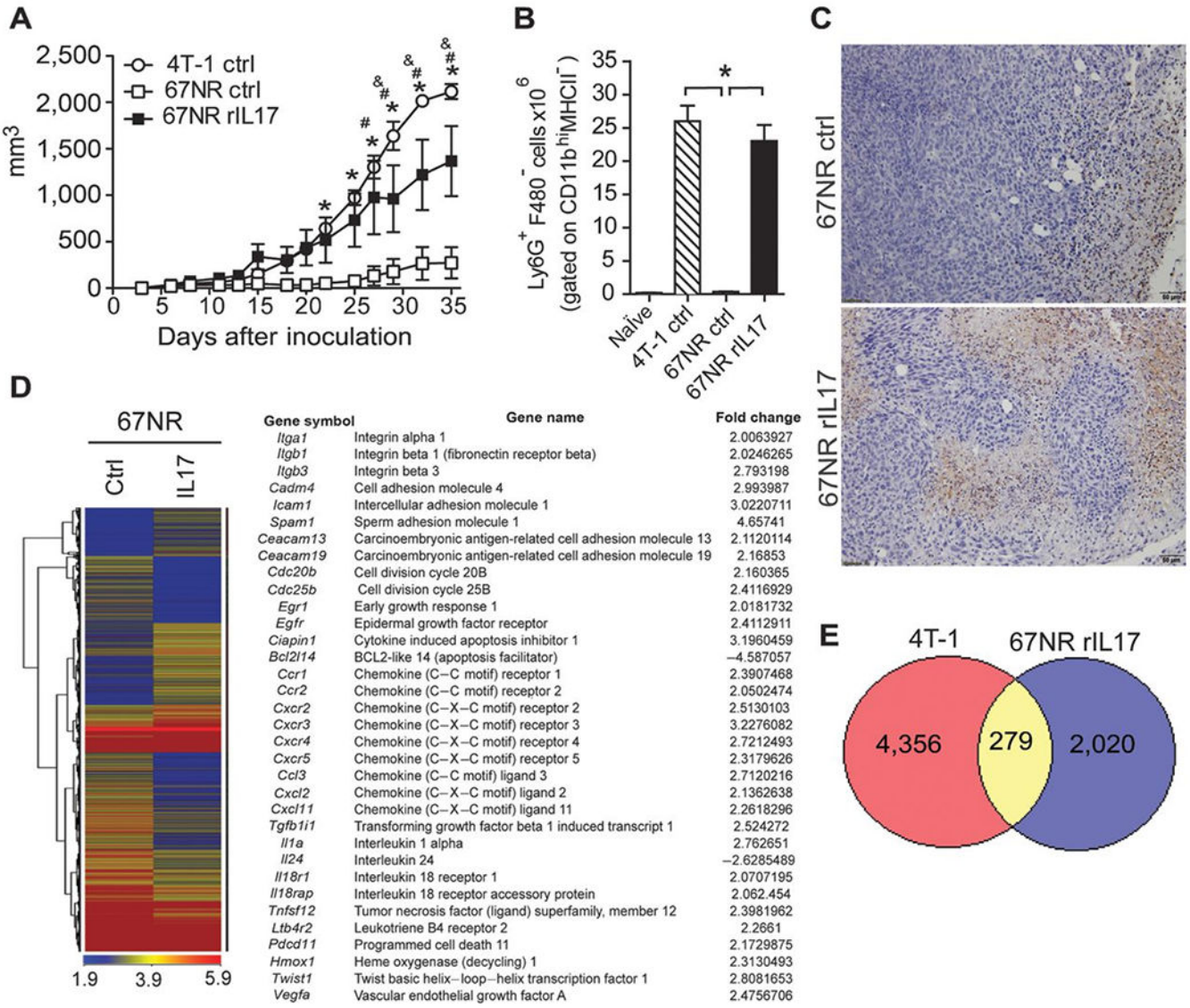

Gene symbol	Gene name	Fold change
Itga1	Integrin alpha 1	2.0063927
Itgb1	Integrin beta 1 (fibronectin receptor beta)	2.0246265
Itgb3	Integrin beta 3	2.793198
Cadm4	Cell adhesion molecule 4	2.993987
Icam1	Intercellular adhesion molecule 1	3.0220711
Spam1	Sperm adhesion molecule 1	4.65741
Ceacam13	Carcinoembryonic antigen-related cell adhesion molecule 13	2.1120114
Ceacam19	Carcinoembryonic antigen-related cell adhesion molecule 19	2.16853
Cdc20b	Cell division cycle 20B	2.160365
Cdc25b	Cell division cycle 25B	2.4116929
Egr1	Early growth response 1	2.0181732
Egfr	Epidermal growth factor receptor	2.4112911
Ciapin1	Cytokine induced apoptosis inhibitor 1	3.1960459
Bcl2l14	BCL2-like 14 (apoptosis facilitator)	−4.587057
Ccr1	Chemokine (C−C motif) receptor 1	2.3907468
Ccr2	Chemokine (C−C motif) receptor 2	2.0502474
Cxcr2	Chemokine (C−X−C motif) receptor 2	2.5130103
Cxcr3	Chemokine (C−X−C motif) receptor 3	3.2276082
Cxcr4	Chemokine (C−X−C motif) receptor 4	2.7212493
Cxcr5	Chemokine (C−X−C motif) receptor 5	2.3179626
Ccl3	Chemokine (C−C motif) ligand 3	2.7120216
Cxcl2	Chemokine (C−X−C motif) ligand 2	2.1362638
Cxcl11	Chemokine (C−X−C motif) ligand 11	2.2618296
Tgfb1i1	Transforming growth factor beta 1 induced transcript 1	2.524272
Il1a	Interleukin 1 alpha	2.762651
Il24	Interleukin 24	−2.6285489
Il18r1	Interleukin 18 receptor 1	2.0707195
Il18rap	Interleukin 18 receptor accessory protein	2.062.454
Tnfsf12	Tumor necrosis factor (ligand) superfamily, member 12	2.3981962
Ltb4r2	Leukotriene B4 receptor 2	2.2661
Pdcd11	Programmed cell death 11	2.1729875
Hmox1	Heme oxygenase (decycling) 1	2.3130493
Twist1	Twist basic helix−loop−helix transcription factor 1	2.8081653
Vegfa	Vascular endothelial growth factor A	2.4756706

Figure 6. IL17A directly affects breast cancer tumor cell behavior *in vivo*.

67NR cells were either treated or not treated with rIL17 *in vitro*, and after 48 hours, these cells were used to inoculate BALB/c mice to induce mammary tumors. A, the volumes of the tumors were measured at 5 dpi and monitored daily. B, at 35 dpi, the numbers of neutrophils ($Ly6G^+F4/80^-$) gated on $CD11b^+MHCII^-$ cells were analyzed in the population of granulocytes isolated from the spleen by flow cytometry. C, immunohistochemical staining in tumor tissues of the mice receiving untreated 67NR cells (top) or treated with rIL17 (bottom) at 35 dpi was used to detect Ly6G protein. The data are representative of two independent experiments with similar results and are shown as the mean ± SEM of four mice per group (*, $P < 0.05$). 67NR cells were either treated or not treated with rIL17. After 48 hours, the mRNA was extracted, and the gene-expression profiles were analyzed by a microarray. D, heat map displaying the hierarchical clustering of the gene-expression profiles. The table presents selected differentially expressed genes of interest. The complete list of the differentially expressed immune response is presented in Supplementary Tables S2

and S3. E, the Venn diagram shows the number of upregulated genes in the 4T-1 cells and IL17-pretreated 67NR cells in relation to the untreated 67NR cells. The intersection of the diagram indicates the number of upregulated genes in common between the 4T-1 and IL17-pretreated 67NR cells.

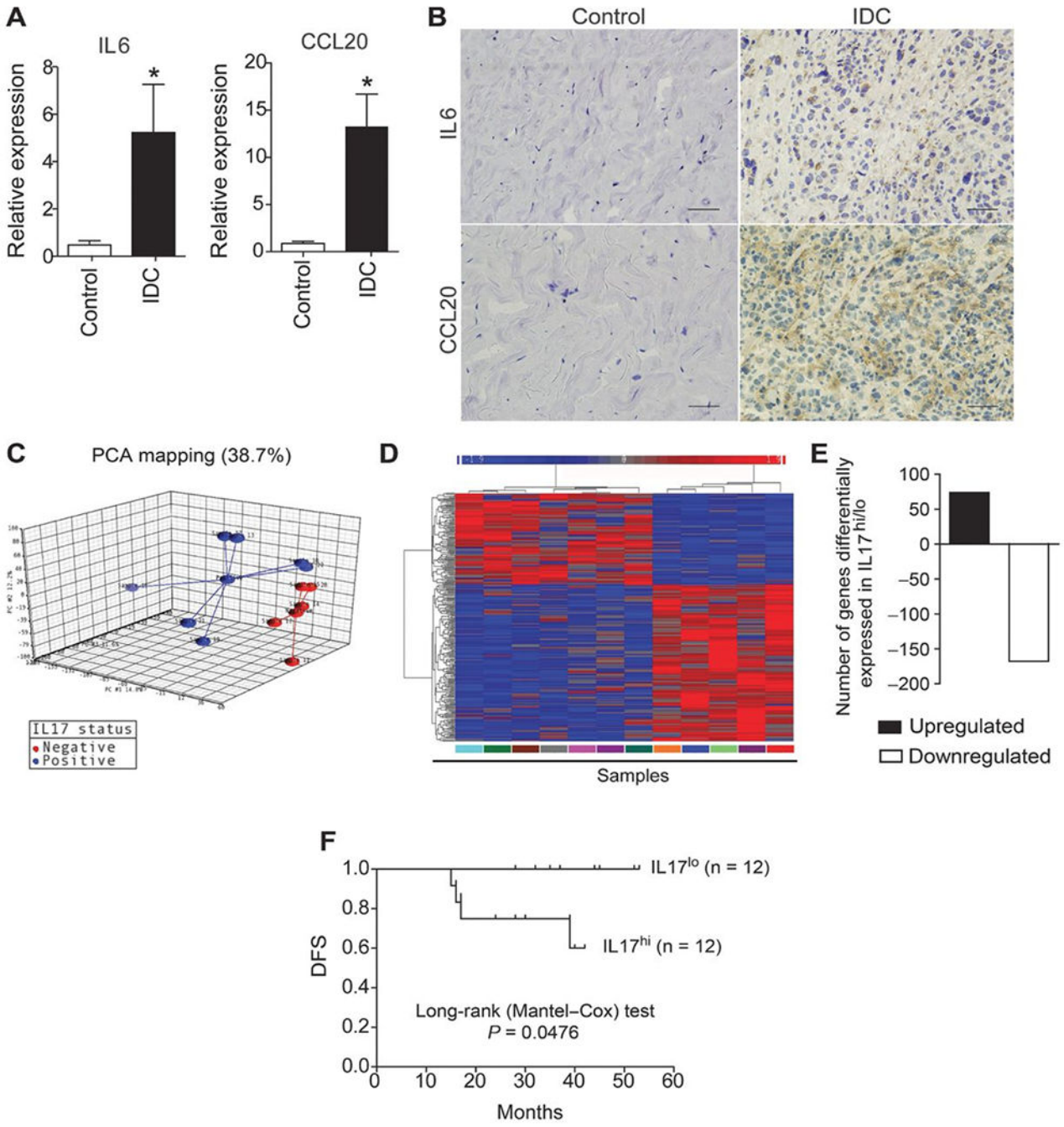

Figure 7. Expression of Th17-promoting cytokines in the tumor microenvironment of patients with IDC.

RNA from breast tumor and healthy control tissue was extracted and analyzed by qPCR. A, the relative expression levels of IL6 and CCL20 are shown. Data are reported as the mean ± SEM of patients ($N = 23$) or healthy control subjects ($N = 8$) who were tested individually. The control values were significantly different compared with those of patients with IDC (*, $P < 0.05$; t test). B, immunohistochemical staining of healthy control (left) and breast tumor tissue (right) was used to detect IL6 and CCL20 protein; scale bars, 50 μm. RNA from breast tumor tissue was extracted, and the gene-expression profiles of samples with low and high

IL17A expression were analyzed by microarray. C, principal component analysis of gene-expression microarray 3D scatter plot showing the first three principal components; each patient sample is connected to a centroid for each group (IL17-positive and IL17-negative). D, heat map showing the hierarchical clustering of the gene-expression profiles of samples with low and high IL17A expression as analyzed by microarray. Values are expressed as the relative units of induction (positive values in red), repression (negative values in blue), and no modulation (gray). E, the bar graph shows the number of genes that were down- and upregulated. F, Kaplan–Meier curves illustrate the DFS of patients according to the expression of IL17A. Log-rank *P* values for the DFS of patients with low and high gene expression were calculated. The data represent the mean ± SEM of 23 patients with IDC (*, $P < 0.05$).